Chemical Methodologies 7(2023) 613-636

Chemical Methodologies

Journal homepage: http://chemmethod.com

Original Research Article

In silico Analysis of Sars-CoV-2 Main Protease Interactions with Selected Hyoscyamus Niger and Datura Stramonium Compounds for Finding New Antiviral Agents

Neda Tadayon[1], Ali Ramazani[1,2,3,4]*

[1]*Department of Chemistry, Faculty of Science, University of Zanjan, Zanjan, Iran*
[2]*Department of Biotechnology, Research Institute of Modern Biological Techniques (RIMBT), University of Zanjan, Zanjan, Iran*
[3]*Department of Agronomy, Research Institute of Modern Biological Techniques (RIMBT), University of Zanjan, Zanjan, Iran*
[4]*Department of Animal Science, Research Institute of Modern Biological Techniques (RIMBT), University of Zanjan, Zanjan, Iran*

ARTICLE INFO

Article history

Submitted: 2023-07-16
Revised: 2023-08-20
Accepted: 2023-08-25
Manuscript ID: CHEMM-2307-1691
Checked for Plagiarism: Yes
Language Editor:
Dr. Fatimah Ramezani
Editor who approved publication:
Dr. Sami Sajjadifar

DOI:10.48309/CHEMM.2023.407403.1691

KEYWORDS

Coronavirus
Hyoscyamus niger
Datura stramonium
Molecular docking
Molecular dynamics simulations

ABSTRACT

So far, many efforts have been made to obtain suitable drugs and vaccines against the new coronavirus. Virtual screening methods are very efficient due to their low cost and high performance, and they are also widely used for designing new herbal medicines. Datura and Hyoscyamus, from the Solanaceae family, have many medicinal properties. This research identified potential compounds from the plants Hyoscyamus niger and Datura stramonium using molecular docking and dynamics studies. These plants have alkaloids, glycosides, terpenoids, steroids, flavonoids, tannins, and saponins. Many of them have attracted significant interest due to their variety of pharmacological activities and may have the potential to cure the new Coronavirus. Therefore, 93 known compounds were investigated, and then five compounds with the lowest binding energies were chosen for docking study. Additionally, atomic molecular dynamics simulation was performed to discover the dynamic behaviour of the main protease (Mpro): ligand complexes. Fraxtin indicated potential activity to inhibit the main protease (Mpro), but further *in vitro*, *in vivo*, and clinical trial studies are needed to confirm this claim.

* Corresponding author: Ali Ramazani
✉ E-mail: aliramazani@znu.ac.ir

GRAPHICAL ABSTRACT

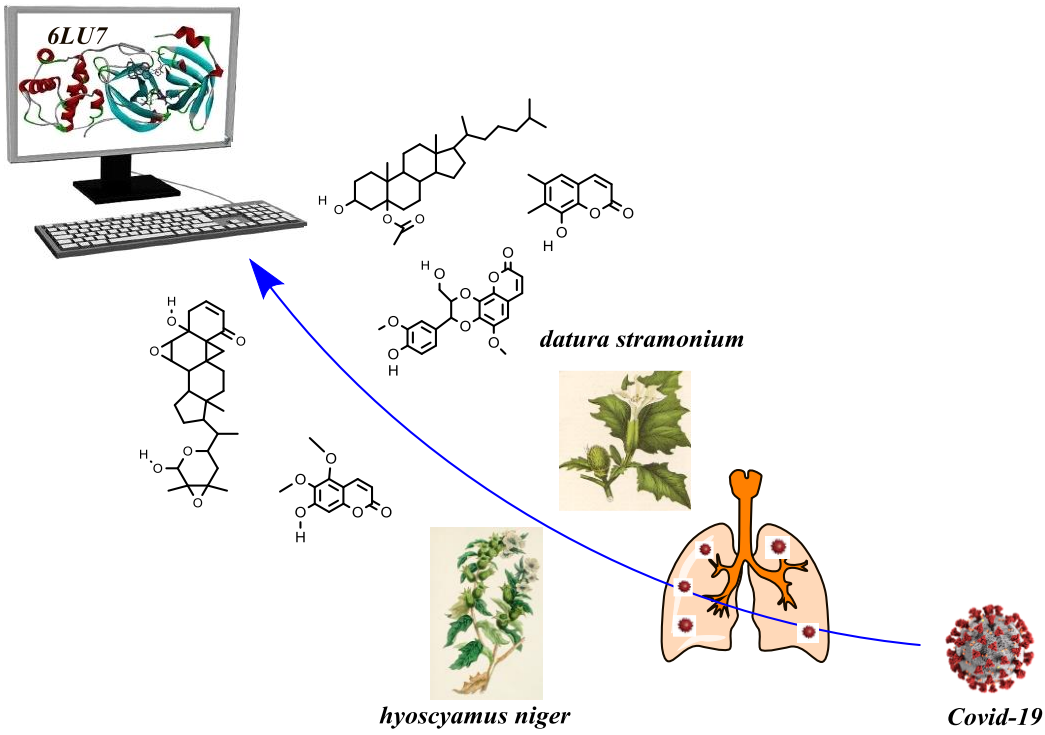

Introduction

In late December 2019, the spread of Coronavirus disease across the globe caused a serious crisis [1,2]. The new coronavirus is seemingly highly pathogenic, contagious, and infectious. In COVID-19, most cases show signs like pyrexia, dry cough, tiredness, sore throat, runny nose, stuffy nose, loss of taste or smell, diarrhea, and digestive tract symptoms, while in a few patients it primarily targets the human respiratory system and causes severe illness [3-6]. This disease has affected the whole world, and by March 2023, it has infected more than 759 million people and caused more than 6 million deaths [7]. Several vaccines against COVID-19 have been quickly developed, such as the inactivated virus COVID-19 vaccine and mRNA vaccines, which have shown effectiveness against the spread of SARS-CoV-2 [8]. However, the fast-evolving variants of the new coronavirus, such as alpha, beta, gamma, theta, kappa, delta, delta-plus, and Omicron, may make these vaccines less effective [9,10]. Thus, we require more potential drugs with better results and fewer side effects to save human society from severely pathogenic Covid-19 strains [11-13]. Targeting viral particles can inhibit SARS-CoV-2 infection, making it the best therapeutic approach [14]. The new coronavirus is a single-stranded RNA with a symmetric helical nucleocapsid that contains four major structural proteins: spike, nucleocapsid, membrane, and coat. Furthermore, this new virus has non-structural proteins such as the main protease of the coronavirus (3CLpro), papain-like (PLpro), and RNA-dependent RNA polymerase (RdRp) [15,16]. The 3CLpro is one of the main proteins that play a vital role in coronavirus replication [17,18]. Since there are no human proteases with a main protease homologue, it is an ideal target for drug design because the inhibitors are less toxicity to humans [19]. In this field, computer-assisted drug design can be used for compounds (FDA-approved drugs or natural products) that have already proven to be safe and effective in humans [20,21]. Computational methods have already provided antiviral compounds against influenza [22], Ebola [23-25], Zika [26-28], Dengue [29-32], and CoVs [33-36] viruses. Natural products are one of the important sources of medicine for the treatment of various illnesses due to their low toxicity and high biological potency [37,38]. Also, natural bioactive molecules derived from plants can be used for the potential treatment of novel coronavirus disease

due to their immunomodulatory, anti-inflammatory, and antioxidant properties [39,40]. The use of natural medicines to treat inflammation in coronavirus disease has reduced the disease progression and the duration of hospitalization [41,42]. The Solanaceae family contains many important pharmaceutical plants, with 98 genera and more than 2700 species [43]. Datura stramonium and Hyoscyamus niger are widespread annual plants from the Solanaceae family [44]. These plants are widely distributed in South America, Central and North America, Africa, Europe, and Asia [45]. They contain some compounds such as alkaloids, glycosides, terpenoids, steroids, flavonoids, tannins, saponins, and anthraquinones compounds [46]. They have shown pharmacological effects such as: antioxidant, antidepressant, anti-inflammatory, antioxidant, antimicrobial, anti-asthmatic, anti-diabetic, anticholinergic, hypotensive, hepatoprotective, and immune-boosting properties, *etc*. [47-49]. To investigate the antiviral effect of natural compounds against the coronavirus 2 main protease (Mpro), we have focused on the natural compounds using a computational approach from Datura stramonium and Hyoscyamus niger. We have performed a screening study on the 93 different known compounds of both plants, and it is found that five ligands (Cleomiscosin A, Cholestane-3,5-diol 5-acetate (3beta,5alpha), Fraxetin, Hyoscyamilactol, and Umckalin) show high interaction with the Mpro. The effect of the elected compounds on the Mpro structure was investigated via molecular dynamics (MD) studies and molecular docking.

Materials and methods

Receptor and ligands selection

In this study, the compounds previously identified in two plants, Datura stramonium and Hyoscyamus niger, were used [44,46]. These ligands were tested against the Mpro [3CLpro (3-chymotrypsin-like protease)] target protein of new coronavirus, which was obtained from the protein data bank (PDB ID: 6LU7). The three-dimensional crystal structure of this new coronavirus is highly significant for viral replication and, due to its differences from human proteases; it could be an excellent target for inhibitory research. The Mpro of the new coronaviruses was detected using the X-ray diffraction technique.

Receptor and ligands preparation

With the Discovery Studio 4.5 software, the inhibitor and water molecules were deleted from Mpro. Using AutoDock Tools 1.5.6, protein optimization was done by adding Kollman partial charges and polar hydrogen atoms. The sizes of the grid box and receptor with a space of 1 Å were chosen based on the dimensions of x, y, and z coordinates during the docking study. To download the structure of the required ligands, we used the PubChem database. Furthermore, to convert the structures into pdb format, we used Biovia Discovery Studio. The PubChem IDs of the ligands obtained in this study are: Cleomiscosin A (CID: 442510), Cholestane-3,5-diol, 5-acetate, (3beta,5alpha) (CID: 91691425), Fraxetin (CID: 5273569), Hyoscyamilactol (CID: 100942617), and Umckalin (CID: 5316862). The ligands were prepared by removing water, adding Gasteiger charges, and setting the number of torsion atoms.

Molecular docking

To observe the binding affinity and protein-ligand docking platform, molecular docking is used to distinguish and evaluate protein-ligand interactions [50]. The binding poses of the ligands in the active site of covid-19 main protease (6LU7) were created with the Auto dock tool (ADT). In this study, the Auto Dock Vina was used to study the 63 compounds in binding to the Mpro. For each ligand, 20 conformations were obtained, and then the top 5 ligands with the lowest binding energy were chosen for flexible molecular docking. Auto Dock Tools, discovery studio and LigPlot+ were used to visualize the docking findings.

Molecular dynamics simulations

The dynamical behavior of 3CLpro and 3CLpro: ligand complexes were explored using all atom

MD simulations as implemented in GROMACS 2019.3 software. Also, The VMD 2.9 program was used to visualize the MD path [51,52]. The initial coordinates of 3CLpro, ligands, and 3CLpro:ligand complexes were calculated by the outputs of the molecular docking method. The AMBER force field gave all bond and non-bond potential energy function parameters for all species. The items required for the MD simulation of the ligands were prepared using the Antechamber program [53]. Next, GROMACS software was used to convert the output files of Antechamber to topology and coordinate compatible files [54]. The restrained electrostatic potential (RESP) approach was used to assign partial charges to ligands and proteins [55]. Short-range non-bonded interactions were modeled using the 12-6 Lennard-Jones potential with a cutoff of 12 Å. The Particle mesh Ewald method was applied to calculate long-range electrostatic interactions, and periodic boundary conditions were applied in all directions. The 3CLpro:ligand complex was placed in the center of a cubic solvation box filled with TIP3P water model, and a solvation shell of 10 Å was applied. The 3CLpro has a negative charge of 4, so 4 sodium ions (Na^+) were added to the simulation box to neutralize the system. Moreover, salt (Na^+Cl^-) with a concentration of 0.145 M was used to more accurately simulate physiological conditions [56]. To reduce thermal noise in the dissolved dendrimers and potential energies, the steepest descent minimization algorithm was used following the conjugate gradient method. The first phase of the equilibrium simulation was used for 500 ps under the canonical (NVT) ensemble to reach the simulation system at 310 K. Next, an isothermal-isobaric equilibrium (NPT) simulation was performed for 1 ns to maintain isotropic pressure at 1 bar. Production MD runs were conducted for 50 ns using the NPT ensemble, and the release of position restraints was performed after completing two equilibration steps.

Results and Discussion

Molecular docking

Docking is applicable for understanding the interactions between the receptor and the ligand, as well as predicting ligand-protein affinity [57]. Blocking the proteases His41 and Cys145 helps reduce virus replication and its impact on the host [58]. Therefore, the main protease 3CLpro of the novel coronavirus was targeted to identify potential compounds that block the His41 and Cys145 catalytic sites. The Cleomiscosin A-Mpro complex exhibited the lowest binding energy of -8.2 kcal/mol and formed four hydrogen bonds with SER144, LEU141, CYS145, GLY143, and π-alkyl interaction with PRO168 and MET165, and five Van der Waals interactions with ASN142, GLN189, THR190, ASP187, and ARG188 (Figure 1).

Fraxetin-Mpro complex indicated the least binding energy of -6.2 kcal/mol. It is characterized by six H-bonding interactions with GLY143, CYS145, SER144, LEU141, HIS163, and GLU166, two Pi-donor bonds with CYS145, GLN189, one Donor-Donor bond with CYS145 and ten Van der Waals interactions with GLN189, MET165, HIS172, HIS163, PHE140, LEU141, SER144, ASN142, LEU27, and HIS41 (Figure 2).

Hyoscyamilactol-Mpro complex have minimum binding energy of -7.3 kcal/mol. Four conventional hydrogen bonds were seen at GLU166, LEU167, GLY143, and CYS145. GLU166, GLN189, HIS164, and ASN142 were seen bonding via carbon hydrogen bond. Nine residues GLN189, MET165, HIS41, THR26, THR25, ASN142, LEU27, CYS145, and LEU167 were observed by Van der Waals bond (Figure 3).

Cholestane-3,5-diol, 5-acetate, (3beta,5alpha)-Mpro complex gave the minimum binding energy of -6.5 kcal/mol. SER144, LEU141, and CYS145 were creating conventional hydrogen bonds. Other interactions were observed with HIS163 and PRO168 residues like Alkyl and Pi-alkyl. GLY143, MET49, HIS41, GLN189, LEU167, THR190, GLU166, MET165, PHE140, ASN142, and SER144 were forming a Van der Waals bond with the ligand (Figure 4).

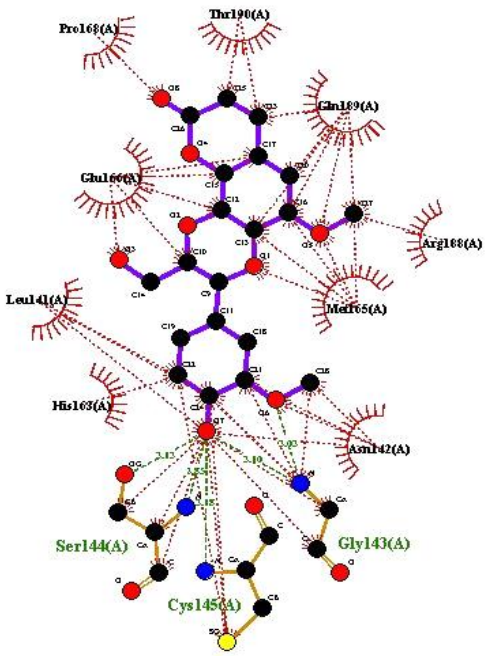

(A)

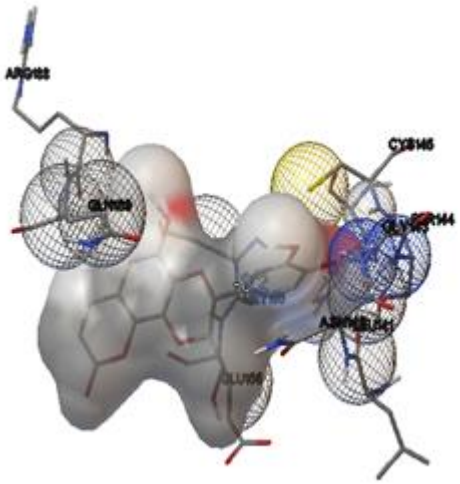

(B)

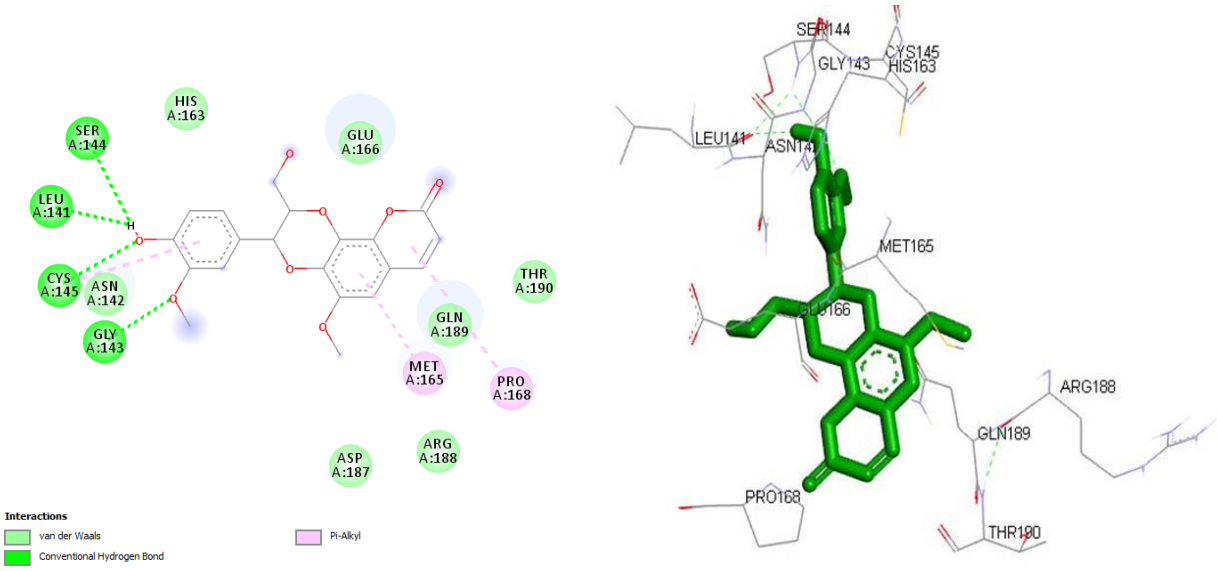

(C)

Figure 1: Interaction of Cleomiscosin A with Mpro: (A) LigPlot+, (B) Auto Dock tools, and (C) 2D and 3D schematic of Discovery studio

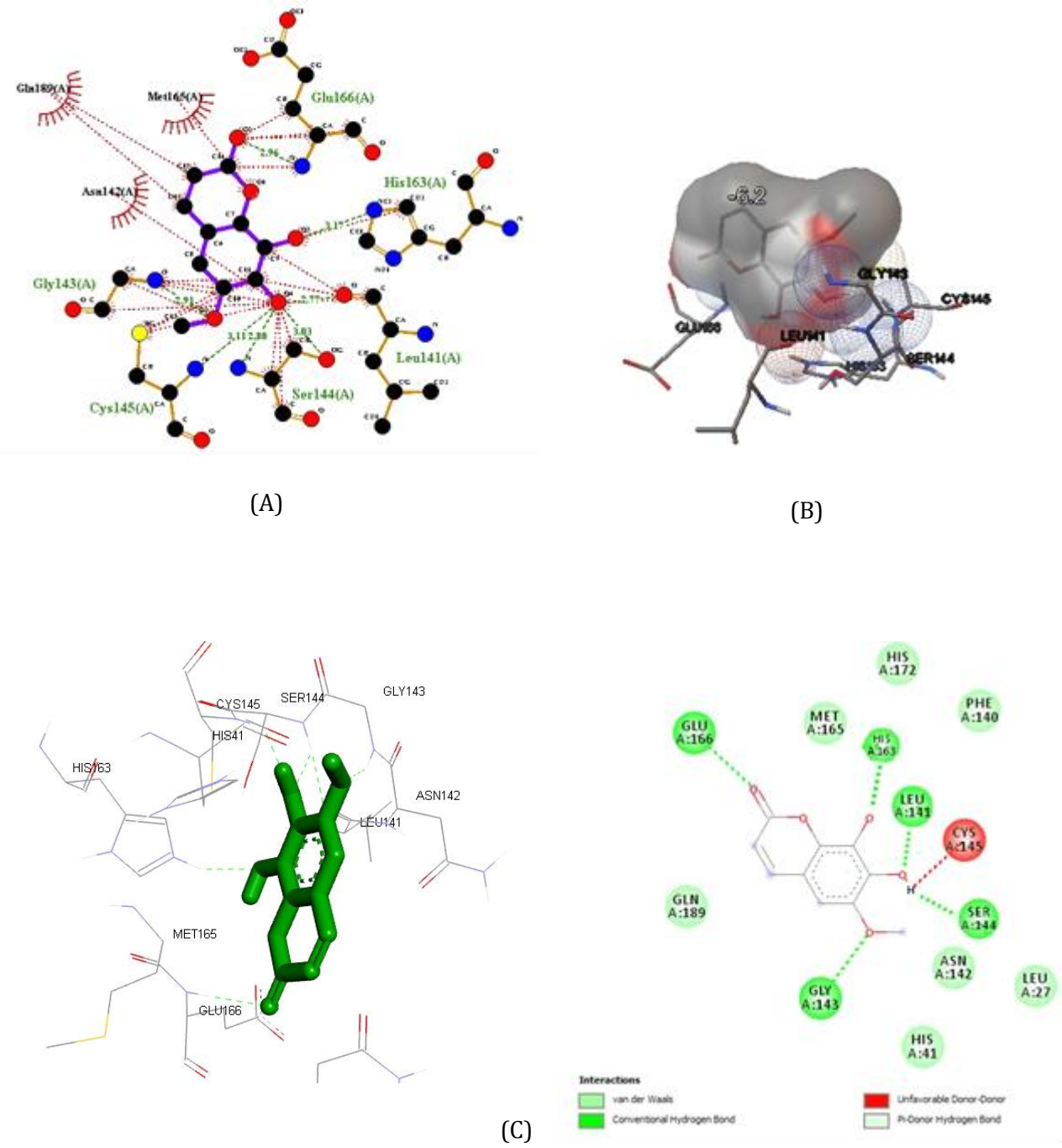

Figure 2: Interaction of Fraxetin with Mpro: (A) LigPlot+, (B) Auto Dock tools, and (C) 3D and 2D schematic of Discovery studio

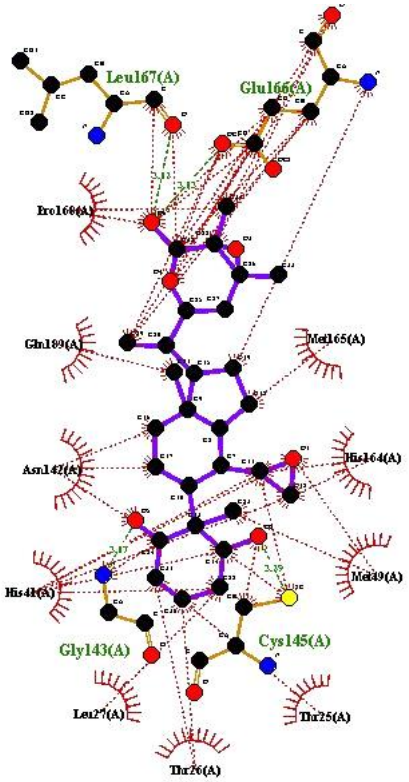

(A)

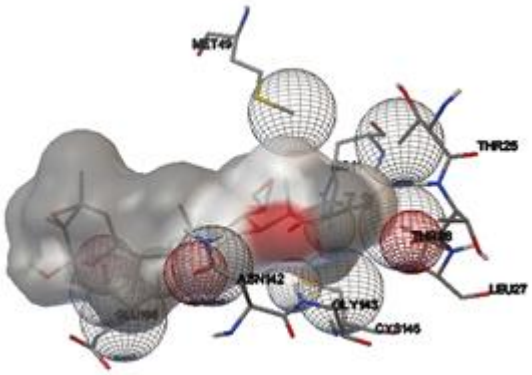

(B)

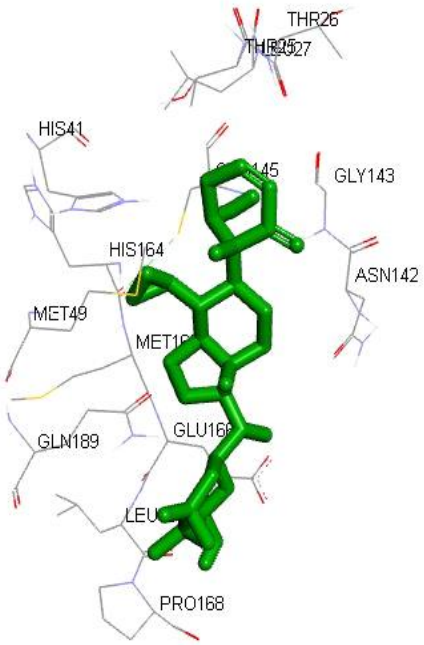

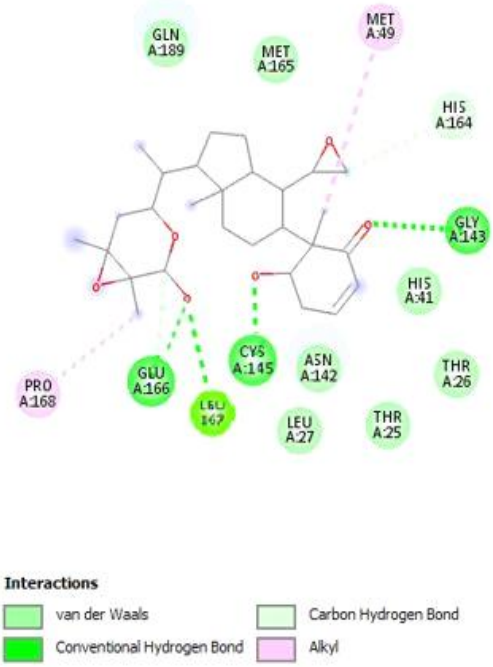

(C)

Figure 3: Interaction of Hyoscyamilactol with Mpro: (A) LigPlot+, (B) Auto Dock tools, and (C) 3D and 2D schematic of Discovery studio

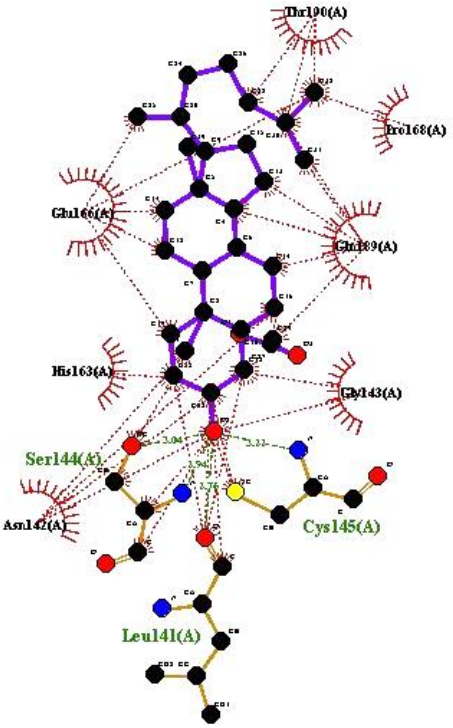

(A)

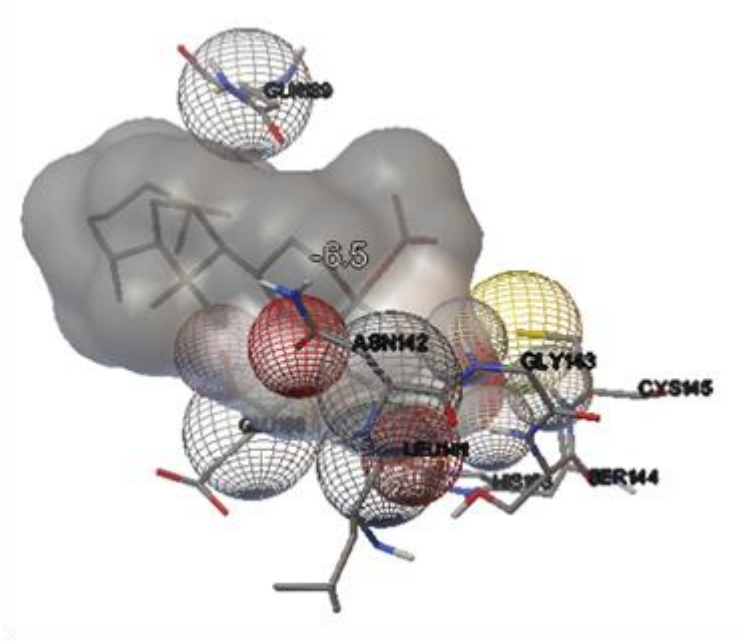

(B)

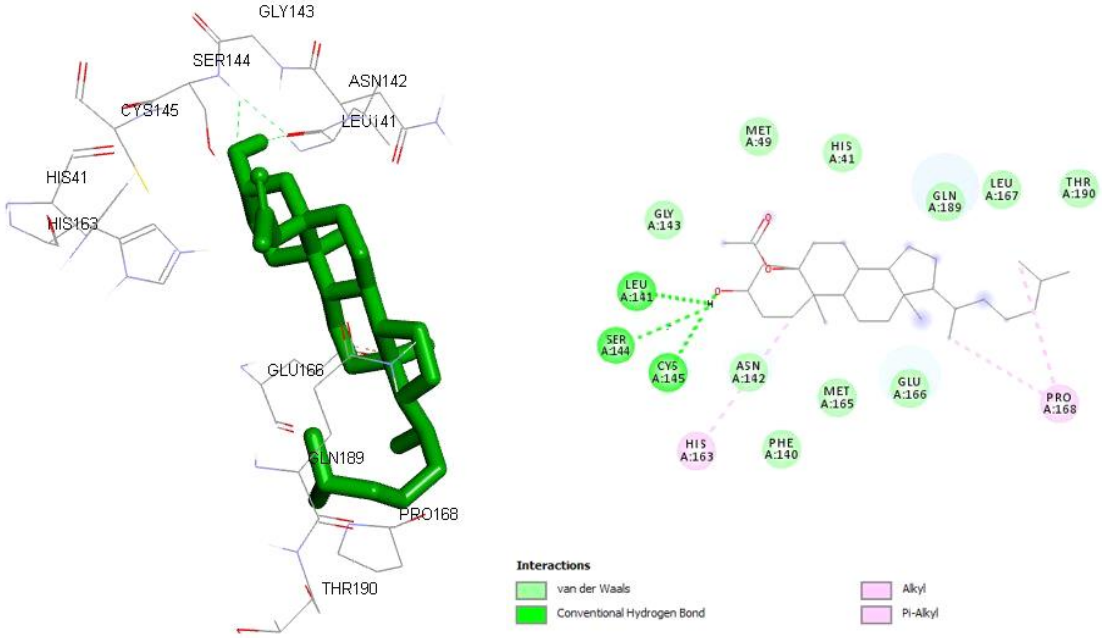

(C)

Figure 4: Interaction of Cholestane-3,5-diol, 5-acetate, (3beta,5alpha) with Mpro: (A) LigPlot+, (B) Auto Dock tools, and (C) 3D and 2D schematic of Discovery studio

Umckalin [7-hydroxy-5,6-dimethoxychromen-2-one]- Mpro complex showed a binding score of -5.7 Kcal/mol. Three sorts of bond formation were seen in the docked complex. CYS145, GLY143, SER144, LEU141, and GLU166 were forming Hydrogen bonds with Umckalin. GLN189, MET49, and ASN142 formed Pi-donor bond with the ligand. Van der Waals bond formation was observed in GLN189, MET49, LEU27, HIS41,

ASN142, PHE140, HIS163, and MET165 (Figure 5, Table 1).

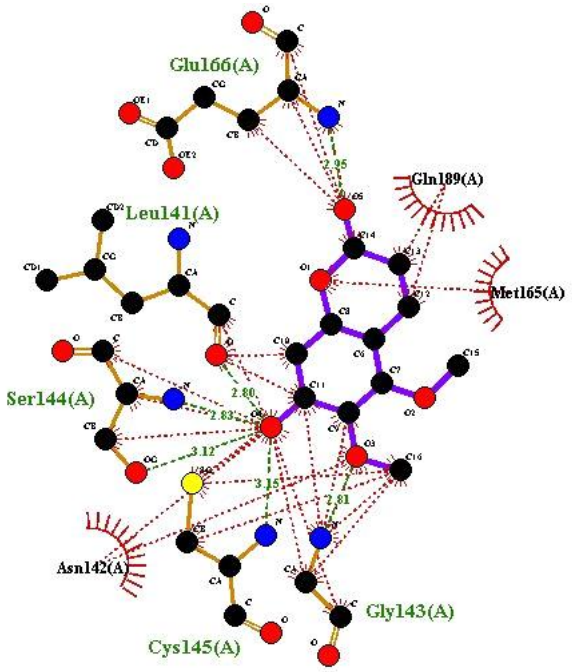

(A)

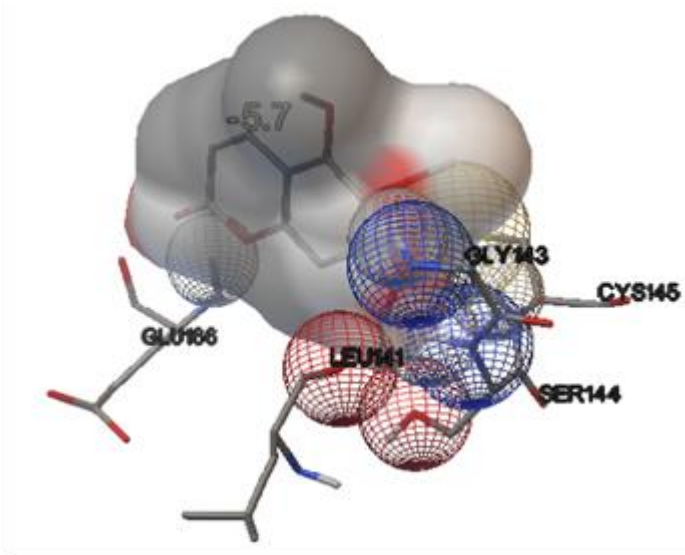

(B)

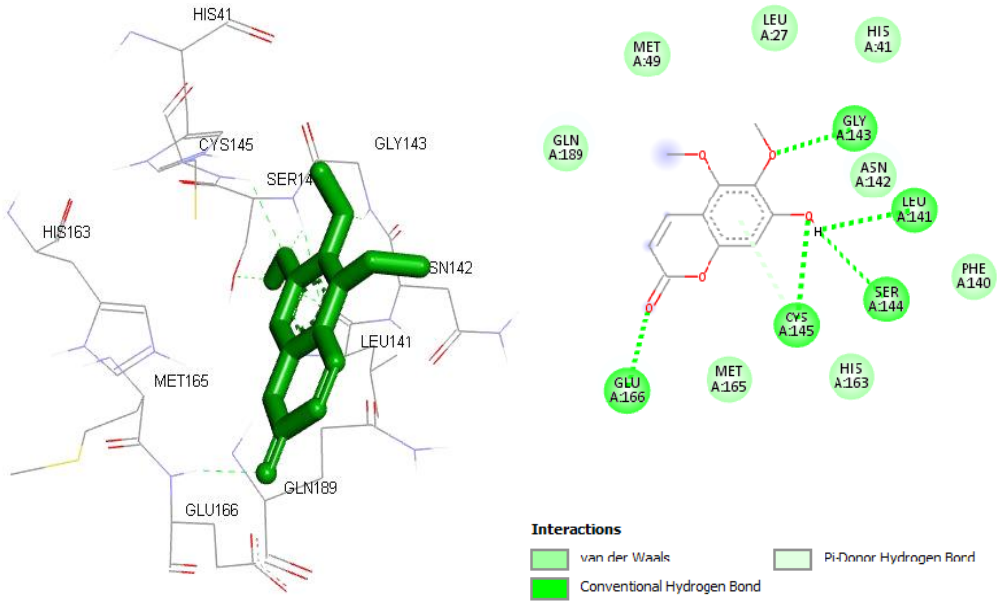

(C)

Figure 5: Interaction of Umckalin with Mpro: (A) LigPlot+, (B) Auto Dock Tools, and (C) 3D and 2D schematic of Discovery studio

Table 1: Interactions and binding energiesof top 5 conformatons of ligands with Mpro

	Compound	Binding energy Kcal/ mol	No. of hydrogen bonds	Hydrogen bond interaction
1	Cleomiscosin A	-8.2	4	LEU141, GLY143 SER144, CYS145
2	Hyoscyamilactol	-7.3	4	CYS145, GLY143, LEU167, GLU166
3	Cholestane-3,5-diol, 5-acetate (3beta,5alpha)	-6.5	3	CYS145, SER144, LEU141
4	Fraxetin	-6.2	6	SER144, CYS145, LEU141, HIS163, GLY143, GLU166
5	Umckalin	-5.7	5	GLY143, GLU166, SER144, CYS145, LEU141

Molecular dynamics (MD) simulations of Mpro-ligand complexes

Molecular dynamics simulations provide us with an in-depth look at the structure of the protein using a number of analysis tools such as radius of gyration (R_g), centre of mass (COM) separation distance between protein and ligands, protein-ligand interaction energies and intermolecular hydrogen bonds, radial distribution functions (RDF), solvent accessible surface area (SASA), root-mean-square fluctuation (RMSF), and root-mean-square deviation (RMSD).

Equilibration and relaxation of protein-ligand complexes

The average distance between the corresponding atoms of the protein backbone through MD simulation run time is referred to as RMSD. According to its definition, RMSD can be used as an indicator of reaching stability and equilibrium during the MD trajectory. Thus, RMSD was chosen as the first criterion to check whether the simulation time is sufficient for sampling. Figure 6 shows the RMSD of atomic positions of 3CLpro backbone calculated against the initial structure of Mpro-Cleomiscosin A, Mpro-Fraxetin, and Mpro-Hyoscyamilactol complexes. The RMSD plot of native Mpro is further represented for comparison. The time series show that the RMSD levels off to almost constant values after about 35 ns of molecular dynamics simulations, indicating that the Mpro structure is well equilibrated and useful information is provided because of the long simulation time on the protein-ligand separation distances, nature of interactions between ligand molecules and protein, microstructure of protein, etc. The mean quantity of root-mean-square deviation is determined to be about 0.30 ± 0.02, 0.22 ± 0.03, 0.23 ± 0.02, and 0.20 ± 0.02 nm for Mpro, Mpro-Cleomiscosin A, Mpro-Fraxetin, and Mpro-Hyoscyamilactol complexes. This shows that the structure of Mpro is very stable in the Mpro-ligand complexes. In this study, to equilibrate all simulated systems, statistics were obtained from the last 10 ns of the MD simulation.

Structural characterization of Mpro-ligand complexes

Figure 7 shows the RMSF of protein residues after fitting to a reference frame (i.e. the time-averaged position of each residue). This parameter determines the flexibility of the protein's building blocks and also identifies the regions of the protein structure that fluctuate the most or the least from their mean structure. The general trend of the RMSF plots for all three complexes is similar to the parent protein. Few residue regions of Cleomiscosin A-Mpro show higher fluctuations compared with Mpro (0-2, 97, 100, 118, 154, 214, and 255) while some other residues of protein are more fluctuated including 47, 76, 137-142, 167-170, 188-196, 305, and 306 residues. Fluctuations of the RMSF plot of Fraxetin-Mpro are generally lower than the reference protein, and this

difference is very evident in the cases of 112-146, 167-171, and 187-203 residue regions. In the case of Hyoscyamilactol-Mpro complex, the only residues that show more fluctuations after interaction with the ligand molecule are 1-3 and 118. The average quantity of root-mean-square fluctuation is determined to be about 0.16, 0.15, 0.13, and 0.14 nm for free Mpro, Cleomiscosin A-Mpro, Fraxetin-Mpro, and Hyoscyamilactol-Mpro, respectively. Thus, binding of these ligands reduces the fluctuation of protein building blocks.

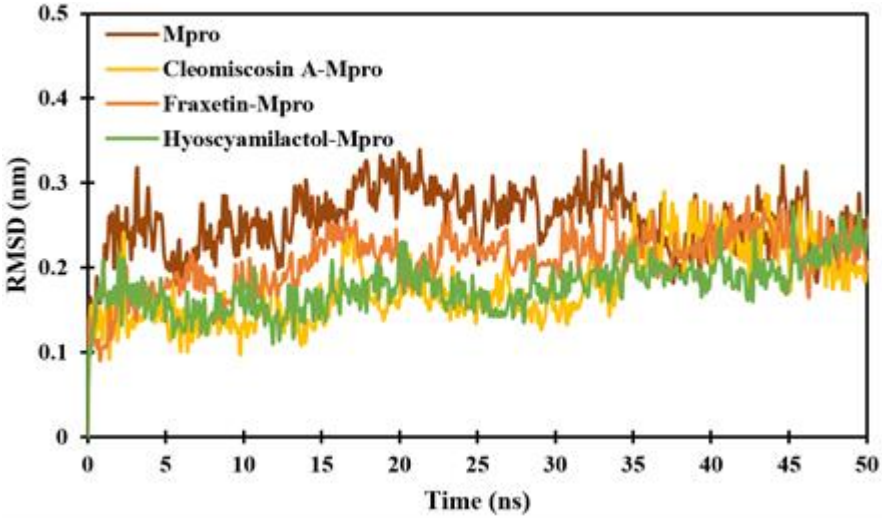

Figure 6: Atom-positional RMSD of the Mpro backbone designated for Mpro, Cleomiscosin A-Mpro, Fraxetin-Mpro, and Hyoscyamilactol-Mpro complexes

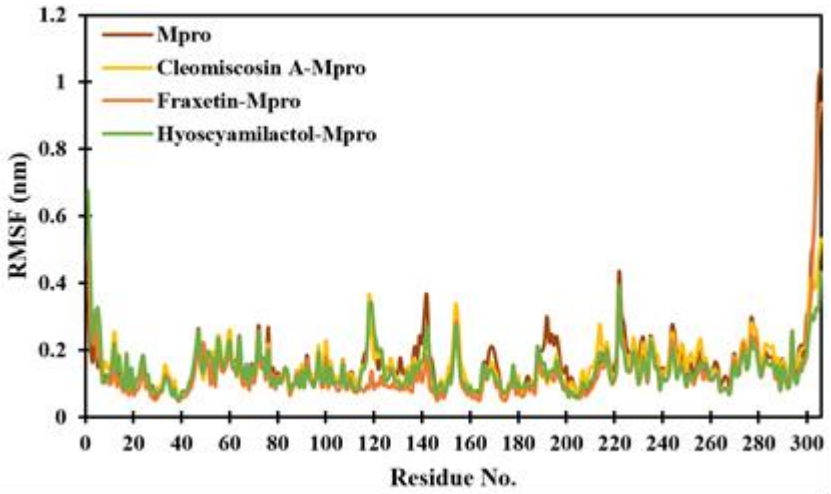

Figure 7: Protein per residue RMSF during production MD run time evaluated for Mpro, Cleomiscosin A-Mpro, Fraxetin-Mpro, and Hyoscyamilactol-Mpro complexes

To determine the preferential binding sites of the ligands within the protein, the equilibrium structures of the protein-ligand complexes at the end of the molecular dynamics (MD) simulations, as well as the amino acid residues distributed within 5 Å of the ligand molecules, are represented in Figures 8 to 10. Figure 8 demonstrates that Cleomiscosin A is surrounded by residues THR45, THR26, LEU27, MET165, THR25, HIS41, CYS44, MET49, CYS145, HIS164, LEU167, VAL186, ASP187, SER46, ARG188, GLN189, THR190, and GLN192. From Figure 9, it can be observed that in the equilibrated structure of Fraxetin-Mpro, amino acids HIS41, THR45, THR25, SER46, GLU47, CYS44, ASP48, MET49, LEU50, ASN51, PRO52, TYR54, ARG188, GLN189, MET165, VAL186, ASP187, and HIS164 surround the ligand.

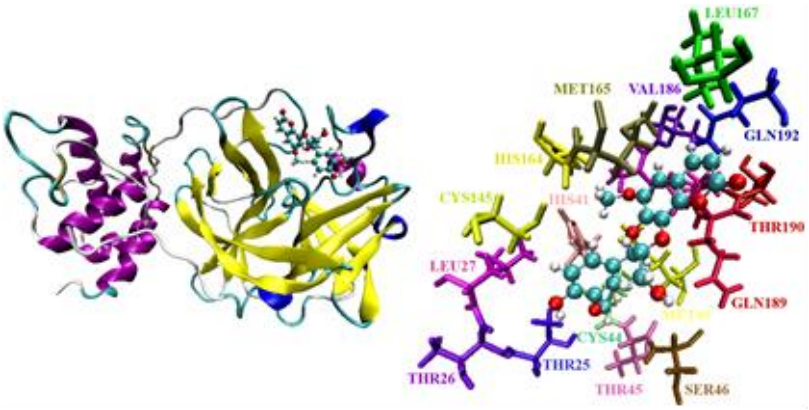

Figure 8: Representation of the equilibrium conformation of Cleomiscosin A-Mpro complex and amino acids that interact with Cleomiscosin A molecule

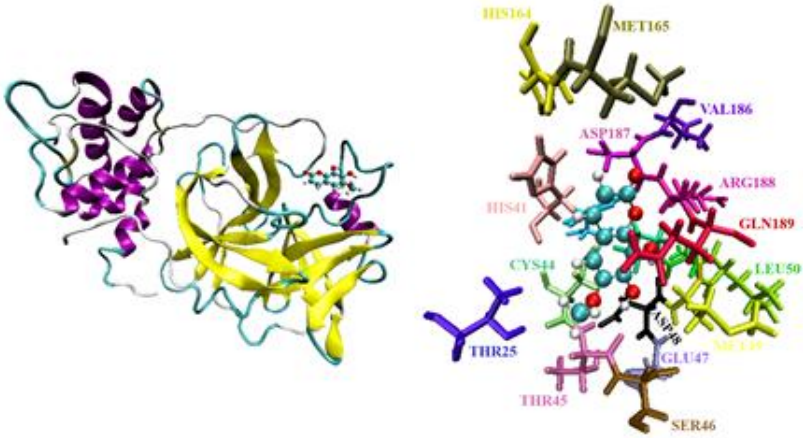

Figure 9: Representation of the equilibrium conformation of Fraxetin-Mpro complex and amino acids that interact with Fraxetin molecule

Finally, Hyoscyamilactol is interacting with amino acids GLU166, THR25, THR26, HIS41, VAL42, CYS145, SER46, GLN189 MET49, ASN142, GLY143, LEU27, HIS163, HIS164, MET165, and THR24 (Figure 10). Thus, all three ligands adopt almost the same binding site in Mpro.

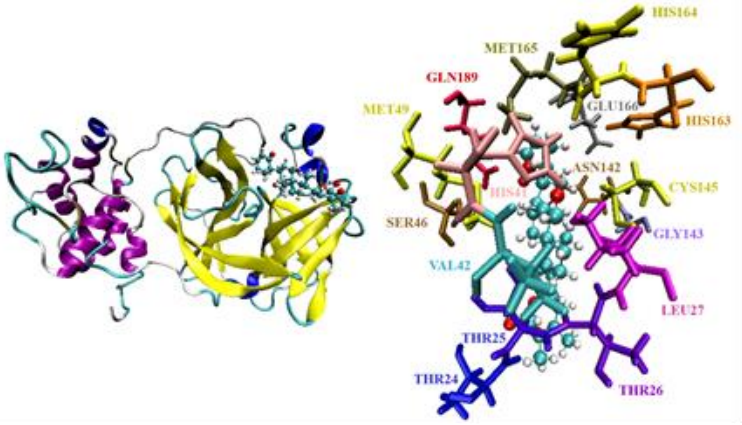

Figure 10: Representation of the equilibrium conformation of Hyoscyamilactol-Mpro complex and amino acids that interact with Hyoscyamilactol molecule

As mentioned earlier, blocking the HIS41 and CYS145 proteases helps to decrease virus replication and its burden on the host. Figure 11 presented the interaction distances between ligand molecules and Mpro extracted using RDF plots of HIS41 and CYS145 to the ligand molecules.

The probability of distribution of B atoms around A ones as reference atoms was evaluated by radial distribution functions. The $g_{A-B}(r)$ is represented by Equation (1):

$$g_{A-B}(r) = \frac{\left(\frac{n_B}{4\pi r^2 \Delta r}\right)}{\left(\frac{N_B}{N}\right)} \quad (1)$$

where, n_B is the number of B atoms distributed around the A atoms in a spherical shell with a Δr thickness. N_B represents the total number of B atoms in an amorphous cell. It can be observed from Figure 11(a) that Fraxetin-HIS41 RDF shows the highest peak, which is mainly distributed at a distance of 0.35-0.52 nm of HIS41 residue of Mpro. This sharp peak indicates that this ligand preserves an almost constant distance from HIS41 during the MD run time. The height of RDF profile of Cleomiscosin A is almost half of that of Fraxetin. Furthermore, in the case of Cleomiscosin A, we observe a distribution zone that starts from 0.30 nm and extends up to 0.60 nm, implying the fluctuation of Cleomiscosin A-HIS41 interaction distance at different MD frames. The weakest and broadest peak is related to Hyoscyamilactol molecule, which indicates the variable distance between the HIS41 and this ligand. Radial pair distribution profiles of CYS145 amino acid to the ligand molecules (Figure 11(b)) are similar for all three ligands, indicating that Cleomiscosin A, Fraxetin, and Hyoscyamilactol molecules are distributed at a distance of 0.50-0.90 nm, 0.55-0.90 nm, and 0.51-0.80 nm from CYS145, respectively. Overall, we conclude that Fraxetin can act as an inhibitor of both HIS41 and CYS145 amino acids.

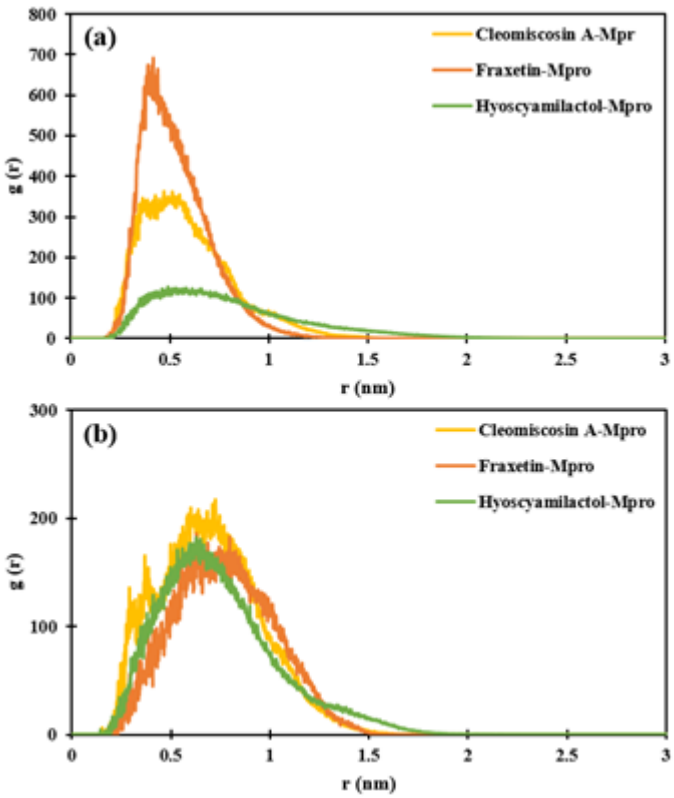

Figure 11: Radial pair distribution profiles of (a) HIS41 and (b) CYS145 amino acids to the ligand molecules

The radius of gyration (Rg) for a protein with an N atom is calculated by Equation (2):

$$R_g^2 = \frac{1}{M}\sum_{k=1}^{N}[m_k(r_k - r_{mean})^2] \quad (2)$$

Where, M is the total mass of protein, N is the number of atoms of protein, m_k is the mass of the kth atom, r_{mean} corresponds to the centre of the protein, and $(r_k - r_{mean})$ is the distance of the kth atom from the centre. The reason behind choosing R_g as an analysis tool is that it enables us to assess the protein compactness so that a stably folded protein preserves a relatively constant value of R_g while the R_g value of an unfolded protein will changes during the MD trajectory [59]. Figure 12 indicates RG as a function of simulation time in unloaded Mpro and also cleomyscosin A-Mpro, Fraxetin-Mpro, and Hyoscyamilactol-Mpro complexes. The average value of RG for free MPRO, Cleomiscosin A-MPRO, Fracastin-mpro, and Hyoscyamilactol-mproS Complexes over the last 10 ns of MD trajectory was approximately 2.21 ± 0.01, 2.26 ± 0.01, 2.21 ± 0.01 nm. It also seems that the radius of gyration value of Mpro remains almost constant upon interaction with Fraxetin and Hyoscyamilactol while Cleomiscosin A causes a slight increase of R_g of Mpro.

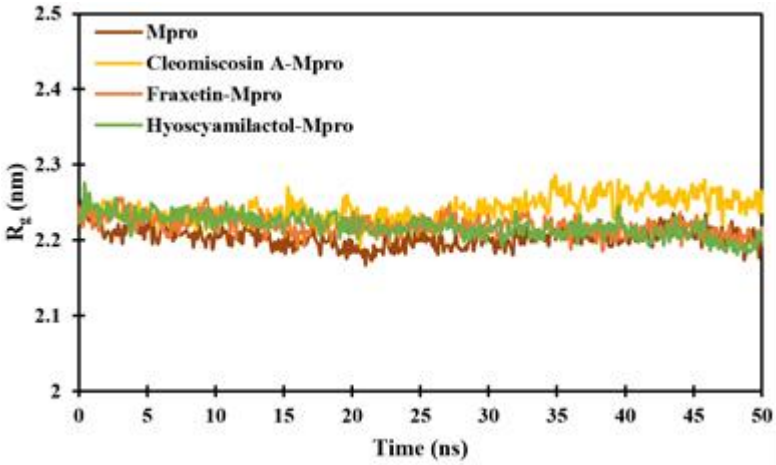

Figure 12: Radius of gyration (R_g) of unloaded Mpro and also Cleomiscosin A-Mpro, Fraxetin-Mpro, and Hyoscyamilactol-Mpro complexes

Hydrogen bond analysis

One of the most important non-covalent interactions in biological systems is hydrogen bonds, which create a dipole- dipole interaction between the hydrogen of an X—H group (X: an electronegative atom) with one or more electronegative atoms [60]. The peptide backbone is made by α helices and β sheets by forming a hydrogen bond between the amine atom and the oxygen atom of the carbonyl group. Therefore, hydrogen bonds play an important role in building the secondary or tertiary structures of proteins. Along the sequence of the same strand in α-helix, hydrogen N-H four residues give hydrogen bond with carbonyl oxygen. Also, hydrogen bonds are created between the appropriate functional groups of various strands of protein in a β-sheet. Therefore, it could be mentioned that the most important interactions in biological systems that create the stability of host-guest complexes are hydrogen bonds. Using the gmx analysis, we investigated the structure of protein-ligand complexes and the contribution of hydrogen bonds in the stability of these complexes. The number of hydrogen bonds formed during 50 ns of MD simulation between Mpro and substrate molecules is depicted in Figure 13. It can also be seen in Figure 13 that during the simulation time, the intermolecular hydrogen bonds are broken several times, especially in the Cleomiscosin A-Mpro complex.

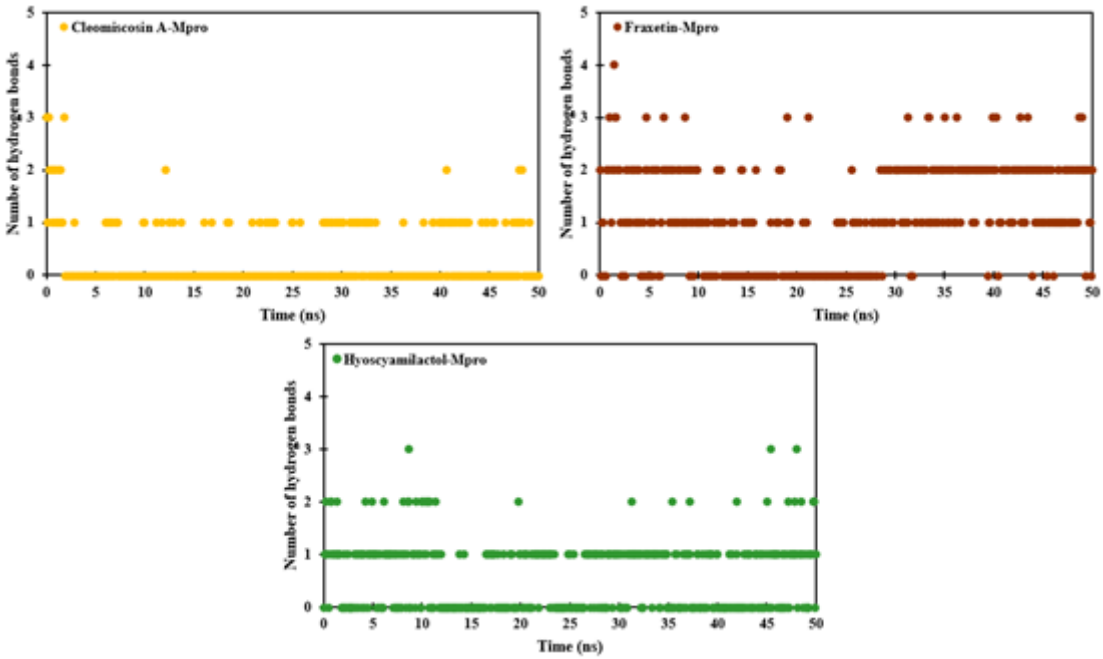

Figure 13: Formation of intermolecular hydrogen bonds (a) Cleomiscosin A, (b) Fraxetin, and (c) Hyoscyamilactol molecules and Mpro

Table 2: The most important hydrogen bond donor and acceptor groups in Cleomiscosin A-Mpro, Fraxetin-Mpro, and Hyoscyamilactol-Mpro complexes

Cleomiscosin A-Mpro		Fraxetin-Mpro		Hyoscyamilactol-Mpro	
Donor—Hydrogen	Acceptor	Donor—Hydrogen	Acceptor	Donor—Hydrogen	Acceptor
HIS41$_{(N-H)}$	Cleomiscosin A_{O1}	ASN142$_{(N-H)}$	Fraxetin$_{O2}$	THR24$_{(O-H)}$	Hydroxytropane$_{O6}$
HIS41$_{(N-H)}$	Cleomiscosin A_{O7}	ASN142$_{(N-H)}$	Fraxetin$_{O5}$	THR26$_{(N-H)}$	Hydroxytropane$_{O1}$
SER46$_{(O-H)}$	Cleomiscosin A_{O8}	GLY143$_{(N-H)}$	Fraxetin$_{O2}$	THR26$_{(N-H)}$	Hydroxytropane$_{O3}$
ASN142$_{(N-H)}$	Cleomiscosin A_{O8}	GLY143$_{(N-H)}$	Fraxetin$_{O4}$	HIS41$_{(N-H)}$	Hydroxytropane$_{O1}$
GLY143$_{(N-H)}$	Cleomiscosin A_{O5}	GLY143$_{(N-H)}$	Fraxetin$_{O5}$	HIS41$_{(N-H)}$	Hydroxytropane$_{O3}$
GLY143$_{(N-H)}$	Cleomiscosin A_{O6}	GLU166$_{(N-H)}$	Fraxetin$_{O1}$	SER46$_{(O-H)}$	Hydroxytropane$_{O1}$
SER144$_{(N-H)}$	Cleomiscosin A_{O5}	GLU166$_{(N-H)}$	Fraxetin$_{O2}$	SER46$_{(O-H)}$	Hydroxytropane$_{O2}$
CYS145$_{(N-H)}$	Cleomiscosin A_{O5}	GLU166$_{(N-H)}$	Fraxetin$_{O3}$	SER46$_{(O-H)}$	Hydroxytropane$_{O3}$
GLN189$_{(N-H)}$	Cleomiscosin A_{O2}	GLU166$_{(N-H)}$	Fraxetin$_{O4}$	SER46$_{(O-H)}$	Hydroxytropane$_{O6}$
GLN189$_{(N-H)}$	Cleomiscosin A_{O3}	GLU166$_{(N-H)}$	Fraxetin$_{O5}$	ASN142$_{(N-H)}$	Hydroxytropane$_{O2}$
GLN189$_{(N-H)}$	Cleomiscosin A_{O4}	ARG188$_{(N-H)}$	Fraxetin$_{O4}$	ASN142$_{(N-H)}$	Hydroxytropane$_{O4}$

GLN189$_{(N-H)}$	Cleomiscosin A$_{O8}$	GLN189$_{(N-H)}$	Fraxetin$_{O3}$	ASN142$_{(N-H)}$	Hydroxytropane$_{O6}$
Cleomiscosin A$_{(O5-H9)}$	HIS41O	GLN189$_{(N-H)}$	Fraxetin$_{O1}$	GLY143$_{(N-H)}$	Hydroxytropane$_{O2}$
Cleomiscosin A (O5–H9)	SER144$_{OG}$	GLN189$_{(N-H)}$	Fraxetin$_{O2}$	GLY143$_{(N-H)}$	Hydroxytropane$_{O3}$
Cleomiscosin A$_{(O8-H18)}$	ASN141$_{OD1}$	GLN189$_{(N-H)}$	Fraxetin$_{O4}$	CYS145$_{(N-H)}$	Hydroxytropane$_{O3}$
Cleomiscosin A$_{(O8-H18)}$	GLU166$_{OE1}$	THR190$_{(N-H)}$	Fraxetin$_{O3}$	GLN189$_{(N-H)}$	Hydroxytropane$_{O1}$
Cleomiscosin A$_{(O8-H18)}$	GLN189$_{OE1}$	GLN192$_{(N-H)}$	Fraxetin$_{O2}$	GLN189$_{(N-H)}$	Hydroxytropane$_{O2}$
		GLN192$_{(N-H)}$	Fraxetin$_{O3}$	GLN189$_{(N-H)}$	Hydroxytropane$_{O3}$
		Fraxetin$_{(O3-H4)}$	HIS41$_{ND1}$	GLN189$_{(N-H)}$	Hydroxytropane$_{O5}$
		Fraxetin$_{(O3-H4)}$	ASP48$_{O}$	Hyoscyamilactol$_{(O3-H27)}$	THR25$_{OG1}$
		Fraxetin$_{(O3-H4)}$	MET49$_{O}$	Hyoscyamilactol$_{(O3-H27)}$	THR26$_{O}$
		Fraxetin$_{(O3-H4)}$	TYR54$_{OH}$	Hyoscyamilactol$_{(O3-H27)}$	HIS41$_{ND1}$
		Fraxetin$_{(O3-H4)}$	HIS164$_{O}$	Hyoscyamilactol$_{(O3-H27)}$	GLN189$_{OE1}$
		Fraxetin$_{(O3-H4)}$	GLU166$_{OE1}$	Hyoscyamilactol$_{(O6-H42)}$	THR26$_{OG1}$
		Fraxetin$_{(O3-H4)}$	GLU166$_{OE2}$	Hyoscyamilactol$_{(O6-H42)}$	GLU166$_{OE1}$
		Fraxetin$_{(O3-H4)}$	GLU166$_{O}$	Hyoscyamilactol$_{(O6-H42)}$	GLU166$_{OE2}$
		Fraxetin$_{(O3-H4)}$	ASP187$_{O}$	Hyoscyamilactol$_{(O6-H42)}$	GLU166$_{O}$
		Fraxetin$_{(O3-H4)}$	ARG188$_{N}$		
		Fraxetin$_{(O3-H4)}$	ARG188$_{O}$		
		Fraxetin$_{(O3-H4)}$	THR190$_{O}$		
		Fraxetin$_{(O4-H5)}$	THR45$_{O}$		
		Fraxetin $_{(O4-H5)}$	ASP48$_{O}$		
		Fraxetin$_{(O4-H5)}$	ASN142$_{OD1}$		
		Fraxetin$_{(O4-H5)}$	ASN142$_{O}$		
		Fraxetin$_{(O4-H5)}$	GLU166$_{OE1}$		
		Fraxetin$_{(O4-H5)}$	GLU166$_{OE2}$		
		Fraxetin$_{(O4-H5)}$	GLU166$_{O}$		
		Fraxetin$_{(O4-H5)}$	ASP187$_{O}$		
		Fraxetin$_{(O4-H5)}$	ARG188$_{O}$		
		Fraxetin$_{(O4-H5)}$	GLN192$_{NE2}$		

Table 2 presents the important donor and acceptor groups of interacting species. According to Figure 13, Fraxetin forms the most number of hydrogen bonds with Mpro. The N—H groups of HIS41, SER46, ASN142, GLY143, SER144, and GLN189 residues act as hydrogen bond donors that interact with oxygens of Cleomiscosin A. On the other hand, the O5—H9 and O8—H18 groups of Cleomiscosin A form intermolecular hydrogen bonds with oxygen atoms of HIS41, SER144, ASN141, GLU166, and GLN189 residues. The N—H groups of ASN142, GLY143, GLU166, ARG188,

GLN189, THR190, and GLN192 are the most important donor groups of protein in Fraxetin-Mpro complex that contribute in hydrogen bonding interactions with oxygen atoms of the ligand. Furthermore, hydroxyl groups of Fraxetin are involved in hydrogen bond interaction with HIS41, ASP48, MET49, TYR54, HIS164, ASP187, GLN192, THR190, THR45, GLU166, ASN142, and ARG188 amino acids. Finally, amine groups of THR26, HIS41, ASN142, GLY143, CYS145, and GLN189 residues as well as hydroxyl groups of THR24 and SER46 form hydrogen bonds with the oxygens of Hyoscyamilactol. The O3—H27 and O6—H42 groups of Hyoscyamilactol interact as donors with oxygen atoms of THR25, THR26, HIS41, GLN189, THR26, and GLU166 of Mpro as acceptors. The average number of hydrogen bonds formed between Mpro and ligands is calculated to be 0.3, 1.1, and 0.6 for Cleomiscosin A, Fraxetin, and Hyoscyamilactol, respectively.

Solvent accessible surface area

The solvation behaviour of a protein is a key factor to consider in evaluation of protein-ligand interactions. The SASA analysis illustrates how many water molecules are accessible by protein amino acids. Therefore, Solvent accessible surface area analysis was performed to evaluate the Mpro ability to do chemistry with solvent and ligand molecules (Figure 14). The average SASA amounts of the protein for the last 10 ns of in this molecular dynamics simulations were evaluated 152 ± 2.5, 153 ± 2.1, 148 ± 1.6, and 149 ± 2.1 nm2 for Mpro, Cleomiscosin A-Mpro, Fraxetin-Mpro, and Hyoscyamilactol-Mpro, respectively. This shows that protein-ligand interactions do not affect the densification of Mpro, significantly.

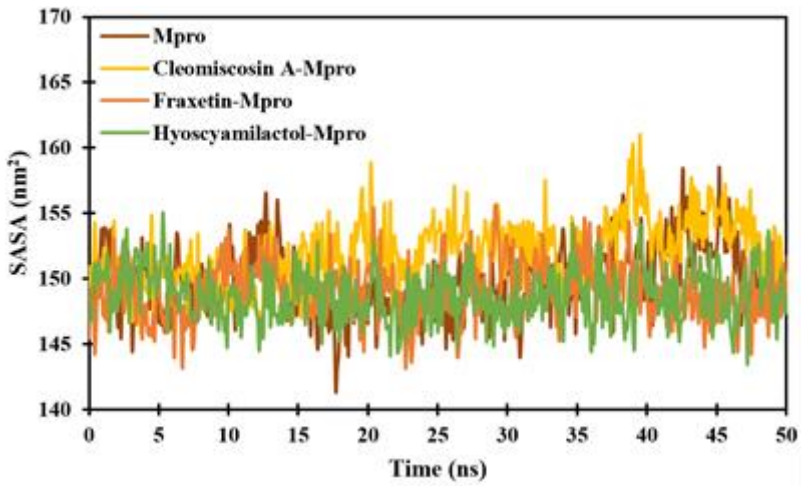

Figure 14: Solvent accessible surface area (SASA) as a function of simulation time for free Mpro and protein in Cleomiscosin A-Mpro, Fraxetin-Mpro, and Hyoscyamilactol-Mpro complexes

The estimated solvation free energies from per exposed surface area are calculated to be -25.0 ± 4.8 $kJ.mol^{-1}.nm^{-2}$ for free Mpro and -30.7 ± 4.6, -31.5 ± 4.6, and -32.3 ± 5.1 $kJ.mol^{-1}.nm^{-2}$ for Cleomiscosin A-Mpro, Fraxetin-Mpro, and Hyoscyamilactol-Mpro complexes, respectively. Figure 15 illustrates the average area over the trajectory per residue for the simulated systems. It can be seen that all simulated systems generally follow a similar trend. Thus, after complex formation, the accessibility of protein residues to the solvent does not change.

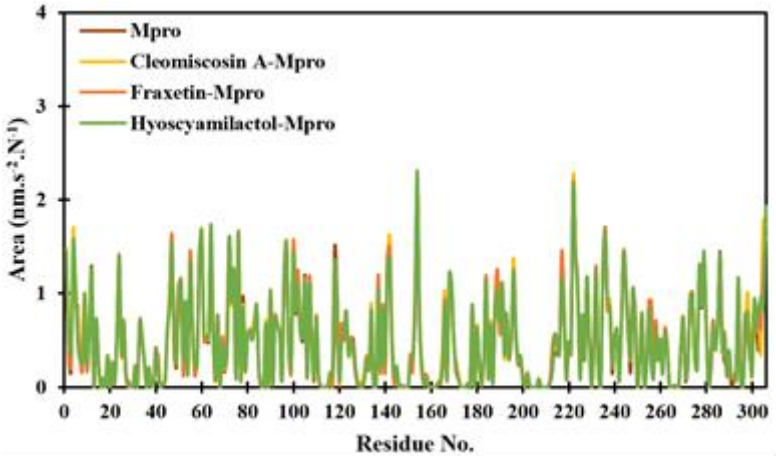

Figure 15: Solvent accessible surface area (SASA) as a function of simulation time for free Mpro and protein in Cleomiscosin A-Mpro, Fraxetin-Mpro, and Hyoscyamilactol-Mpro complexes

Protein-ligand interaction energies

The value of the protein-ligand short-range non-bonded interaction energies was calculated to quantify the strength of the interaction between these two species. The average short-range Coulombic, Lennard-Jones (LJ), and total interaction energies are given in Table 3. The LJ short-range interaction energies show the following trend: Fraxetin > Cleomiscosin A > Hyoscyamilactol. However, the highest value of Coulomb energy belongs to the Hyoscyamilactol-Mpro interactions (-33.1 kJ.mol^{-1}). The strength of Coulomb energies for Cleomiscosin A-Mpro and Fraxetin-Mpro is almost the same. The calculated protein-ligand interaction energies indicate that Fraxetin makes an extremely more stable complex with Mpro than the other two ligands. The obtained result is consistent with the hydrogen bond analysis.

Table 3: The average values of protein-ligand interaction energies (kJ.mol^{-1}) during the MD simulations

Complex	Coulomb energy	LJ energy	Total energy
Cleomiscosin A-Mpro	-23.4	-130.2	-153.6
Fraxetin-Mpro	-25.4	-183.5	-208.9
Hyoscyamilactol-Mpro	-33.4	-119.1	-152.5

Using computational methods to find antiviral drugs is one of the most powerful techniques to fight this disease. Natural compounds have been widely investigated. In a previous study, Elena Campione et al reported the moleculars docking of Umckalin and Fraxetin on the 3CL protease (ID: 6LU7), bovine lactoferrin (ID: 1BLF), spike glycoprotein and catalytic subunit of the RdRp polymerase (ID: 7BV2). The Interaction Energy of Umckalin and Fraxetin on the 3CL protease was -5.7 and -6.9 kcal/mol, respectively. They investigated only compounds with energies higher than -7.5 kcal/mol through molecular dynamics simulations [61]. Abha et al showed that Cleomiscosin A has binding capability with cluster of differentiation molecules (CDs), toll-like receptors (TLR-4) and and inducible nitric oxide synthase (iNOS) protein [62]. Jehoshaphat Oppong Mensah et al researched about interaction of Cleomiscosin A with 6WNP Main Protease of SARS-CoV-2 and they reported the MD simulations of this compound [63]. Also, Gédéon N. Bongo et al stated that the Cleomiscosin A has good binding energy with 6LU7. They noted this compound has higher binding affinity (-8.2) with 3CLpro than Azithromycin but they have not investigated the MD simulations properties of this compound [64]. Olfa Tabbene et al investigated the effects of 12 -hydroxydaturametelin B and Daturametelin B in these plants on interleukin-6"IL-6",tumor necrosis factor-α

"TNF-α", their receptors (TNFR1 and IL-6R) and

both TNF-TNFR1 and IL-6-IL-6R complexes. The infection caused by Covid-19 can increase the levels of cytokines and increase the severity of the disease [65]. Anupam Bishayee et al stated that 12-deoxywithastramonolide, Daturalactone and Daturilin bind with lectin-like oxidized low-density lipoprotein receptor-1 (LOX-1), nuclear factor-κB (NF-κB), inducible nitric oxide synthases (iNOS), cyclooxygenase-1(COX-1) and COX-2. These compounds have the anti-inflammatory effects [66]. Other studies were reported about the other compounds in different plants [67-74]. There have been no studies on Hyoscyamilactol and Cholestane-3,5-diol 5-acetate (3beta,5alpha) interaction with the 3CL main protease of SARS-CoV-2. In this study, the antiviral potency of Cleomiscosin A, Cholestane-3,5-diol 5-acetate (3beta,5alpha), Fraxetin, Hyoscyamilactol and Umckalin against 3CLpro of Sars-CoV-2 were investigated by molecular docking analysis and molecular dynamics simulations.

Conclusion

For confronting the Sars-CoV-2 Virus many studies are targeting to find antiviral treatments. Antiviral potency of Hyoscyamus niger and Datura stramonium compounds against 3CLpro of Sars-CoV-2 were investigated by molecular docking analysis. Five compounds have been indicated the least binding energies and Fraxetin resulted the best potency against of new Coronavirus Mpro (-6.2 Kcal/mol) due to greater numbers of hydrogen bindings.

All molecular dynamics (MD) simulations were used to explore the dynamical aspects of protein-ligand complexes' interactions. The average RMSD values are calculated to be approximately 0.30 ± 0.02, 0.22 ± 0.03, 0.23 ± 0.02, and 0.20 ± 0.02 nm for Mpro, Mpro-Cleomiscosin A, Mpro-Fraxetin, and Mpro-Hyoscyamilactol, respectively, showing that the structure of Mpro is very stable in the Mpro-ligand complexes. The mean quantity of RMSF was obtained to be about 0.16, 0.15, 0.13, and 0.14 nm for free Mpro, Cleomiscosin A-Mpro, Fraxetin-Mpro, and Hyoscyamilactol-Mpro, respectively. Thus, the binding of these ligands reduces the fluctuation of protein building blocks. The height and sharpness of radial pair distribution functions (RDF) peaks suggest that Fraxetin can act as an inhibitor of both HIS41 and CYS145 amino acids. The average number of hydrogen bonds formed between Mpro and ligands is calculated to be 0.3, 1.1, and 0.6 for Cleomiscosin A, Fraxetin, and Hyoscyamilactol, respectively. The average short-range Coulombic, Lennard-Jones (LJ), and total interaction energies of Cleomiscosin A-Mpro (-23.4, -130.2, and -153.6 $kJ.mol^{-1}$, respectively), Fraxetin-Mpro (-25.4, -183.5, and -208.9 $kJ.mol^{-1}$, respectively), and Hyoscyamilactol-Mpro (-33.4, -119.1, and -152.5 $kJ.mol^{-1}$, respectively) show that Fraxetin makes an extremely more stable complex with Mpro in comparison Cleomiscosin A and Hyoscyamilactol.

Disclosure Statement

No potential conflict of interest was reported by the authors.

Funding

This research did not receive any specific grant from funding agencies in the public, commercial, or not-for-profit sectors.

Authors' Contributions

All authors contributed to data analysis, drafting, and revising of the paper and agreed to be responsible for all the aspects of this work

ORCID

Ali Ramazani
https://orcid.org/0000-0003-3072-7924

References

[1]. Kirby T., New variant of SARS-CoV-2 in UK causes surge of COVID-19, *The Lancet Respiratory Medicine*, 2021, **9**:e20 [Crossref], [Google scholar], [Publisher]

[2]. Khan Z., Muhammad K., Ahmed A., Rahman H., Coronavirus outbreaks: prevention and management recommendations, *Drugs & Therapy Perspectives*, 2020, **36**:215 [Crossref], [Google scholar], [Publisher]

[3]. Ye Z.W., Yuan S., Yuen K.S., Fung S.Y., Chan C.P., Jin D.Y., Zoonotic origins of human coronaviruses,

International journal of biological sciences, 2020, **16**:1686 [Crossref], [Google scholar], [Publisher]

[4]. Mengist H.M., Dilnessa T., Jin T., Structural basis of potential inhibitors targeting SARS-CoV-2 main protease, *Frontiers in Chemistry*, 2021, **9**:622898 [Crossref], [Google scholar], [Publisher]

[5]. Habas K., Nganwuchu C., Shahzad F., Gopalan R., Haque M., Rahman S., Majumder A.A., Nasim T., Resolution of coronavirus disease 2019 (COVID-19), *Expert review of anti-infective therapy*, 2020, **18**:1201 [Crossref], [Google scholar], [Publisher]

[6]. Tarique M., Ahmad S., Malik A., Ahmad I., Saeed M., Almatroudi A., Qadah T., Murad M.A., Mashraqi M., Alam Q., Al-Saleh Y., Novel severe acute respiratory syndrome coronavirus 2 (SARS-CoV2) and other coronaviruses: a genome-wide comparative annotation and analysis, *Molecular and Cellular Biochemistry*, 2021, **476**:2203 [Crossref], [Google scholar], [Publisher]

[7]. WHO. WHO Coronavirus Disease (COVID-19) Dashboard. Available online: (accessed on 14 March 2023) [Publisher]

[8]. Ndwandwe D., Wiysonge C.S., COVID-19 vaccines, *Current opinion in immunology*, 2021, **71**:111 [Crossref], [Google scholar], [Publisher]

[9]. COVID U., About Variants of the Virus that Causes COVID-19, 2021 [Google scholar], [Publisher]

[10]. Lauring A.S., Hodcroft E.B., Genetic variants of SARS-CoV-2—what do they mean?, *Jama*, 2021, **325**:529 [Crossref], [Google scholar], [Publisher]

[11]. Ahn D.G., Shin H.J., Kim M.H., Lee S., Kim H.S., Myoung J., Kim B.T., Kim S.J., Current status of epidemiology, diagnosis, therapeutics, and vaccines for novel coronavirus disease 2019 (COVID-19), *Journal of Microbiology and Biotechnology*, 2020, **30**:313 [Crossref], [Google scholar], [Publisher]

[12]. Wang C., Horby P.W., Hayden F.G., Gao G.F., A novel coronavirus outbreak of global health concern, *The lancet*, 2020, **395**:470 [Crossref], [Google scholar], [Publisher]

[13]. Mirtaleb M.S., Mirtaleb A.H., Nosrati H., Heshmatnia J., Falak R., Emameh R.Z., Potential therapeutic agents to COVID-19: An update review on antiviral therapy, immunotherapy, and cell therapy, *Biomedicine & Pharmacotherapy*, 2021, **138**:111518 [Crossref], [Google scholar], [Publisher]

[14]. Sattari A., Ramazani A., Aghahosseini H., Repositioning therapeutics for COVID-19: virtual screening of the potent synthetic and natural compounds as SARS-CoV-2 3CLpro inhibitors, *Journal of the Iranian Chemical Society*, 2021, **18**:2807 [Crossref], [Google scholar], [Publisher]

[15]. Benarba B., Pandiella A., Medicinal plants as sources of active molecules against COVID-19, *Frontiers in pharmacology*, 2020, **11**:1189 [Crossref], [Google scholar], [Publisher]

[16]. Chen Y., Guo Y., Pan Y., Zhao Z.J., Structure analysis of the receptor binding of 2019-nCoV, *Biochemical and Biophysical Research Communications*, 2020, **525**:135 [Crossref], [Google scholar], [Publisher]

[17]. Anand K., Ziebuhr J., Wadhwani P., Mesters J.R., Hilgenfeld R., Coronavirus main proteinase (3CLpro) structure: basis for design of anti-SARS drugs, *Science*, 2003, **300**:1763 [Crossref], [Google scholar], [Publisher]

[18]. Mirza M.U., Froeyen M., Structural elucidation of SARS-CoV-2 vital proteins: Computational methods reveal potential drug candidates against main protease, Nsp12 polymerase and Nsp13 helicase, *Journal of pharmaceutical analysis*, 2020, **10**:320 [Crossref], [Google scholar], [Publisher]

[19]. Wu F., Zhao S., Yu B., Chen Y.M., Wang W., Song Z.G., Hu Y., Tao Z.W., Tian J.H., Pei Y.Y., Yuan M.L., A new coronavirus associated with human respiratory disease in China, *Nature*, 2020, **579**:265 [Crossref], [Google scholar], [Publisher]

[20]. Hassan H.A., Abdelmohsen U.R., Aly O.M., Desoukey S.Y., Mohamed K.M., Kamel M.S., Potential of Ficus microcarpa metabolites against SARS-CoV-2 main protease supported by docking studies, *Natural Product Research*, 2022, **36**:994 [Crossref], [Google scholar], [Publisher]

[21]. Venkatesan P., Repurposing drugs for treatment of COVID-19, *The Lancet Respiratory Medicine*, 2021, **9**:e63 [Crossref], [Google scholar], [Publisher]

[22]. Du J., Cross T.A., Zhou H.X., Recent progress in structure-based anti-influenza drug design, *Drug discovery today*, 2012, **17**:1111 [Crossref], [Google scholar], [Publisher]

[23]. Madrid P.B., Chopra S., Manger I.D., Gilfillan L., Keepers T.R., Shurtleff A.C., Green C.E., Iyer L.V., Dilks H.H., Davey R.A., Kolokoltsov A.A., A systematic screen of FDA-approved drugs for inhibitors of biological threat agents, *PloS one*, 2013, **8**:e60579 [Crossref], [Google scholar], [Publisher]

[24]. Mirza M.U., Ikram N., Integrated computational approach for virtual hit identification against ebola viral proteins VP35 and VP40, *International journal of molecular sciences*, 2016, **17**:1748 [Crossref], [Google scholar], [Publisher]

[25]. Shurtleff A.C., Nguyen T.L., Kingery D.A., Bavari S., Therapeutics for filovirus infection: traditional approaches and progress towards in silico drug design, *Expert opinion on drug discovery*, 2012, **7**:935 [Crossref], [Google scholar], [Publisher]

[26]. ul Qamar Muhammad Tahir, Kiran S., Ashfaq U.A., Javed M.R., Anwar F., Ali, M.A., Gilani, Anwar ul Hassan, Discovery of novel dengue NS2B/NS3 protease inhibitors using pharmacophore modeling and molecular docking based virtual screening of the zinc database, *International Journal of Pharmacology*, 2016, **12**:621 [Google scholar]

[27]. Nitsche C., Strategies towards protease inhibitors for emerging flaviviruses, *Dengue and Zika: control and antiviral treatment strategies*, 2018, 175–186, [Crossref], [Google scholar], [Publisher]

[28]. Pattnaik A., Palermo N., Sahoo B.R., Yuan Z., Hu D., Annamalai A.S., Vu H.L., Correas I., Prathipati P.K., Destache C.J., Li Q., Discovery of a non-nucleoside RNA polymerase inhibitor for blocking Zika virus replication through in silico screening, *Antiviral Research*, 2018, **151**:78 [Crossref], [Google scholar], [Publisher]

[29]. Leela S.L., Srisawat C., Sreekanth G.P., Noisakran S., Yenchitsomanus P.T., Limjindaporn T., Drug repurposing of minocycline against dengue virus infection, *Biochemical and biophysical research communications*, 2016, **478**:410 [Crossref], [Google scholar], [Publisher]

[30]. Luzhkov V., Decroly E., Canard B., Selisko B., Åqvist J., Evaluation of adamantane derivatives as inhibitors of dengue virus mRNA cap methyltransferase by docking and molecular dynamics simulations, *Molecular informatics*, 2016, **32**:155 [Crossref], [Google scholar], [Publisher]

[31]. Wang Q.Y., Patel S.J., Vangrevelinghe E., Xu H.Y., Rao R., Jaber D., Schul W., Gu F., Heudi O., Ma N.L., Poh M.K., A small-molecule dengue virus entry inhibitor, *Antimicrobial agents and chemotherapy*, 2009, **53**:1823 [Crossref], [Google scholar], [Publisher]

[32]. ul Qamar M.T., Mumtaz A., Ashfaq U.A., Adeel M.M., Fatima T., Potential of plant alkaloids as dengue ns3 protease inhibitors: Molecular docking and simulation approach, *Bangladesh Journal of Pharmacology,* 2014, **9**:262 [Crossref], [Google scholar], [Publisher]

[33]. Ramajayam Tan K.P., Liu H.G., Liang P.H., Synthesis, docking studies, and evaluation of pyrimidines as inhibitors of SARS-CoV 3CL protease, *Bioorganic & medicinal chemistry letters*, 2010, **20**:3569 [Crossref], [Google scholar], [Publisher]

[34]. Wang L., Bao B.B., Song G.Q., Chen C., Zhang X.M., Lu W., Wang Z., Cai Y., Li S., Fu S., Song F.H., Discovery of unsymmetrical aromatic disulfides as novel inhibitors of SARS-CoV main protease: chemical synthesis, biological evaluation, molecular docking and 3D-QSAR study, *European journal of medicinal chemistry*, 2017, **137**:450 [Crossref], [Google scholar], [Publisher]

[35]. Wu C., Liu Y., Yang Y., Zhang P., Zhong W., Wang Y., Wang Q., Xu Y., Li M., Li X., Zheng M., Analysis of therapeutic targets for SARS-CoV-2 and discovery of potential drugs by computational methods, *Acta Pharmaceutica Sinica B*, 2020, **10**:766 [Crossref], [Google scholar], [Publisher]

[36]. ul Qamar M.T., Alqahtani S.M., Alamri M.A., Chen L.L., Structural basis of SARS-CoV-2 3CLpro and anti-COVID-19 drug discovery from medicinal plants, *Journal of pharmaceutical analysis*, 2020, **10**:313 [Crossref], [Google scholar], [Publisher]

[37]. Zarei A., Ramazani A., Pourmand S., Sattari A., Rezaei A., Moradi S., In silico evaluation of COVID-19 main protease interactions with honeybee natural products for discovery of high potential antiviral compounds, *Natural product research*, 2022, **36**:4254 [Crossref], [Google scholar], [Publisher]

[38]. Bazyari-Delavar S., Badalkhani-Khamseh F., Ebrahim-Habibi A., Hadipour N.L., PAMAM and polyester dendrimers as favipiravir nanocarriers: a comparative study using DFT method, *Journal of Nanoparticle Research*, 2021, **23**:231 [Crossref], [Google scholar], [Publisher]

[39]. Huang F., Li Y., Leung E.L.H.. Liu X., Liu K., Wang Q., Lan Y., Li X., Yu H., Cui L., Luo H., A review of therapeutic agents and Chinese herbal medicines against SARS-CoV-2 (COVID-19), *Pharmacological research*, 2020, **158**:104929 [Crossref], [Google scholar], [Publisher]

[40]. Trivedi P., Abbas A., Lehmann C., Rupasinghe H.V., Antiviral and anti-inflammatory plant-derived bioactive compounds and their potential use in the treatment of COVID-19-related pathologies, *Journal of Xenobiotics*, 2022, **12**:289 [Crossref], [Google scholar], [Publisher]

[41]. Patel V.K., Shirbhate E., Patel P., Veerasamy R., Sharma P.C., Rajak H., Corticosteroids for treatment of COVID-19: Effect, evidence, expectation and extent, *Beni-Suef University Journal of Basic and Applied Sciences*, 2021, **10**:78, [Crossref], [Google scholar], [Publisher]

[42]. Liu Y.X.; Zhou Y.H.; Jiang C.H., Liu J., Chen D.Q., Prevention, treatment and potential mechanism of herbal medicine for Corona viruses: A review, *Bioengineered*, 2022, **13**:5480 [Crossref], [Google scholar], [Publisher]

[43]. Guha S., Maheshwari S.C., Cell division and differentiation of embryos in the pollen grains of Datura in vitro, *Nature*, 1966, **212**:97 [Crossref], [Google scholar], [Publisher]

[44]. Li J., Shi J., Yu X., Sun J., Men Q., Kang T., Chemical and pharmacological researches on Hyoscyamus niger, *Chinese Herbal Medicines*, 2011, 117-126 [Google scholar], [Publisher]

[45]. Gaire B.P., Subedi L., A review on the pharmacological and toxicological aspects of Datura stramonium L, *Journal of integrative medicine*, 2013, **11**:73 [Crossref], [Google scholar], [Publisher]

[46]. Al-Snafi A.E., Chemical constituents and pharmacological effects of Dalbergia sissoo-A review, *IOSR Journal of Pharmacy*, 2017, **7**:59 [Crossref], [Google scholar]

[47]. Al-Snafi A.E., Phytochemical constituents and medicinal properties of Digitalis lanata and Digitalis purpurea-A review, *Indo American Journal of Pharmaceutical Sciences*, 2017, **4**:225 [Crossref], [Google scholar], [Publisher]

[48]. De-la-Cruz I.M., Hallab A., Olivares-Pinto U., Tapia-López R., Velázquez-Márquez S., Piñero D., Oyama K., Usadel B., Núñez-Farfán J., Genomic signatures of the evolution of defence against its natural enemies in the poisonous and medicinal plant Datura stramonium (Solanaceae), *Scientific Reports*, 2021, **11**:882 [Crossref], [Google scholar], [Publisher]

[49]. İnci Ş., Sancar P.Y., Demirpolat A., Kirbag S., Civelek S., Chemical compositions of essential oils, antimicrobial effect and antioxidant activity studies of Hyoscyamus niger L. from Turkey, *bioRxiv*, 2022 [Crossref], [Google scholar], [Publisher]

[50]. Verdonk M.L., Cole J.C., Hartshorn M.J., Murray C.W., Taylor R.D., Improved protein–ligand docking using GOLD, Proteins: Structure, *Function, and Bioinformatics*, 2003, **52**:609 [Crossref], [Google scholar], [Publisher]

[51]. Van Der Spoel D., Lindahl E., Hess B., Groenhof G., Mark A.E., Berendsen H.J., GROMACS: fast, flexible, and free, *Journal of computational chemistry*, 2005, **26**:1701 [Crossref], [Google scholar], [Publisher]

[52]. Humphrey W., Dalke A., Schulten K., VMD: visual molecular dynamics, *Journal of molecular graphics*, 1996, **14**:33 [Crossref], [Google scholar], [Publisher]

[53]. Wang J., Wang W., Kollman P.A., Case D.A., Automatic atom type and bond type perception in molecular mechanical calculations, *Journal of molecular graphics and modelling*, 2006, **25**:247 [Crossref], [Google scholar], [Publisher]

[54]. Sousa da Silva A.W., Vranken W.F., ACPYPE-Antechamber python parser interface, *BMC research notes*, 2012, **5**:367 [Crossref], [Google scholar], [Publisher]

[55]. Wang J., Cieplak P., Kollman P.A., How well does a restrained electrostatic potential (RESP) model perform in calculating conformational energies of organic and biological molecules?, *Journal of computational chemistry*, 2000, **21**:1049 [Crossref], [Google scholar], [Publisher]

[56]. Esfandiarpour R., Badalkhani-Khamseh F., Hadipour N.L., Exploration of phosphorene as

doxorubicin nanocarrier: An atomistic view from DFT calculations and MD simulations, *Colloids and Surfaces B: Biointerfaces*, 2022, **215**:112513 [Crossref], [Google scholar], [Publisher]

[57]. Gupta M., Sharma R., Kumar A., Docking techniques in pharmacology: How much promising? *Computational biology and chemistry*, 2018, **76**:210 [Crossref], [Google scholar], [Publisher]

[58]. Báez-Santos Y.M., John S.E.S., Mesecar A.D., The SARS-coronavirus papain-like protease: structure, function and inhibition by designed antiviral compounds, *Antiviral research*, 2015, **115**:21 [Crossref], [Google scholar], [Publisher]

[59]. Sahebi U., Gholami H., Ghalandari B., Badalkhani-khamseh F., Nikzamir A., Divsalar A., Evaluation of BLG ability for binding to 5-FU and Irinotecan simultaneously under acidic condition: A spectroscopic, molecular docking and molecular dynamic simulation study, *Journal of Molecular Liquids*, 2021, **344**:117758 [Crossref], [Google scholar], [Publisher]

[60]. Silverman R.B., Holladay M.W., *The organic chemistry of drug design and drug action*, Academic press, 2014 [Google scholar], [Publisher]

[61]. Iacovelli F., Costanza G., Romeo A., Cosio T., Lanna C., Bagnulo A., Di Maio U., Sbardella A., Gaziano R., Grelli S., Squillaci E., Interaction of Pelargonium sidoides compounds with lactoferrin and SARS-CoV-2: insights from molecular simulations. *International journal of environmental research and public health*, 2022, **19**:5254 [Crossref], [Google scholar], [Publisher]

[62]. Meena A., Yadav D.K., Srivastava A., Khan F., Chanda D., Chattopadhyay S.K., In Silico Exploration of Anti- Inflammatory Activity of Natural Coumarinolignoids, *Chemical biology & drug design*, 2011, **78**:567 [Crossref], [Google scholar], [Publisher]

[63]. Mensah J.O., Ampomah G.B., Gasu E.N., Adomako A.K., Menkah E.S., Borquaye L.S., Allosteric Modulation of the Main Protease (MPro) of SARS‐CoV‐2 by Casticin—Insights from Molecular Dynamics Simulations, Chemistry Africa, 2022, **5**:1305 [Crossref], [Google scholar], [Publisher]

[64]. Mulongo E.K., Kilembe J.T., Bongo G.N., Dinangayi D.T., Tshibangu D.S.T., Mpiana P.T., In silico screening of natural compounds from Jatropha curcas (Euphorbiaceae, Linn) and Jatropha gossypifolia (Euphorbiaceae, Linn) against SARS-CoV2, a COVID-19 main protease, using molecular docking approach, *IJFAC (Indonesian Journal of Fundamental and Applied Chemistry)*, 2022, **7**:148 [Google scholar], [Publisher]

[65]. Damergi B., Essid R., Fares N., Khadraoui N., Ageitos L., Ben Alaya A., Gharbi D., Abid I., Rashed Alothman M., Limam F., Rodríguez J., Datura stramonium Flowers as a Potential Natural Resource of Bioactive Molecules: Identification of Anti-Inflammatory Agents and Molecular Docking Analysis, *Molecules*, 2023, **28**:5195 [Crossref], [Google scholar], [Publisher]

[66]. Chandan G., Kumar C., Chibber P., Kumar A., Singh G., Satti N.K., Gulilat H., Saini A.K., Bishayee A., Saini R.V., Evaluation of analgesic and anti-inflammatory activities and molecular docking analysis of steroidal lactones from Datura stramonium L, *Phytomedicine*, 2021, **89**:153621 [Crossref], [Google scholar], [Publisher]

[67]. Mengist H.M., Khalid Z., Adane F., In silico Screening of Potential SARS-CoV-2 Main Protease Inhibitors from Thymus schimperi, *Advances and Applications in Bioinformatics and Chemistry*, 2023, **2023**:1 [Crossref], [Google scholar], [Publisher]

[68]. Rohoullah F., Mitra A., Identification of Potential Anti-COVID-19 Drug Leads from Medicinal Plants through Virtual High-Throughput Screening, *Chemistry open*, 2023, **8**:e202203865 [Crossref], [Google scholar], [Publisher]

[69]. Bárbara Longhini G., Natalia Castelhano de O., Mariane Roberta R., Fernanda Stumpf T., Eduardo Borges M., Andréia Cristina Conegero S., Fernando F.L., Marcus Vinícius P., Jo˜ao Carlos Palazzo de M., Danielly C., Daniela Cristina de Medeiros A., The naturally-derived alkaloids as a potential treatment for COVID-19: A scoping review, *Phytotherapy Research*, 2022, **36**:2686 [Crossref], [Google scholar], [Publisher]

[70]. Selvaraj C., Dinesh D.C., Pedone E.M., Alothaim A.S., Vijayakumar R., Rudhra O., Singh

S.K., SARS-CoV-2 ORF8 dimerization and binding mode analysis with class I MHC: computational approaches to identify COVID-19 inhibitors, *Briefings in Functional Genomics*, 2023, **22**:227 [Crossref], [Google scholar], [Publisher]

[71]. Mosquera-Yuqui F., Lopez-Guerra N., Moncayo-Palacio E.A., Targeting the 3CLpro and RdRp of SARS-CoV-2 with phytochemicals from medicinal plants of the Andean Region: molecular docking and molecular dynamics simulations, *Journal of Biomolecular Structure and Dynamics*, 2022, **40**:2010 [Crossref], [Google scholar], [Publisher]

[72]. Dos Santos Correia P.R., Donato De Souza A.H., Chaparro R.A., Tenorio Barajas A.Y., Porto S.R., Molecular docking, ADMET analysis and molecular dynamics (MD) simulation to identify synthetic isoquinolines as potential inhibitors of SARS-CoV-2 MPRO, *Current Computer - Aided Drug Design*, 2023, **19**:391 [Crossref], [Google scholar], [Publisher]

[73]. Paul G.K., Mahmud S., Aldahish A.A., Afroze M., Biswas S., Gupta S.B.R., Razu M.H., Zaman S., Uddin M.S., Nahari M.H., Alshahrani M.M., Computational screening and biochemical analysis of Pistacia integerrima and Pandanus odorifer plants to find effective inhibitors against Receptor-Binding domain (RBD) of the spike protein of SARS-Cov-2, *Arabian Journal of Chemistry*, 2022, **15**:103600 [Crossref], [Google scholar], [Publisher]

[74]. Biswas S., Mahmud S., Mita M.A., Afrose S., Hasan M.R., Sultana Shimu M., Saleh M.A., Mostafa-Hedeab G., Alqarni M., Obaidullah A.J., Batiha G.E.S., Molecular docking and dynamics studies to explore effective inhibitory peptides against the spike receptor binding domain of SARS-CoV-2, *Frontiers in Molecular Biosciences*, 2022, **8**:791642 [Crossref], [Google scholar], [Publisher]

HOW TO CITE THIS ARTICLE

Neda Tadayon, Ali Ramazani. *In silico* Analysis of Sars-CoV-2 Main Protease Interactions with Selected Hyoscyamus Niger and Datura Stramonium Compounds for Finding New Antiviral Agents. C*hem. Methodol.*, 2023, 7(8) 613-636
DOI: https://doi.org/10.48309/CHEMM.2023.407403.1691
URL: https://www.chemmethod.com/article_178141.html